Experimental Thermal and Fluid Science 98 (2018) 195–205

Contents lists available at ScienceDirect

Experimental Thermal and Fluid Science

journal homepage: www.elsevier.com/locate/etfs

Gas-liquid flow of sub-millimeter bubbles at low void fractions: Void fraction prediction using drift-flux model

Sotiris P. Evgenidis, Thodoris D. Karapantsios*

Department of Chemical Technology and Industrial Chemistry, Faculty of Chemistry, Aristotle University, University Box 116, 541 24 Thessaloniki, Greece

ARTICLE INFO

Keywords:
Drift-flux model
Homogeneous flow
Void fraction
Bubble size
Drift velocity

ABSTRACT

Drift-flux model is a simple and reliable tool for void fraction prediction in two-phase flows. This work examines its performance in gas-liquid flow of small bubbles (< 1 mm) at low void fractions ($< 10^{-1}$) that resembles bubbly flow in human bloodstream during Decompression Sickness and can be also found in other two-phase applications such as flow boiling in macro-channels. Drift-flux model predictions are compared with experimental data measured in co-current upward bubbly flow for varying gas/liquid flow properties. Water and blood simulant are used as test liquids, while bubble size is controlled using prescribed surfactant (SDS) concentrations. Homogeneous flow model, which is a sub-case of drift-flux model, predicts adequately void fraction in water and blood simulant when the mean bubble size is lower than 200 μm. For larger bubbles in water (mean size up to 800 μm) and in blood simulant (mean size up to 350 μm), the performance of thirteen drift-flux models from literature is examined. Ten of them concern specifically bubbly flow, whereas three models are applicable to a wide range of flow conditions. To our knowledge, this is the first time that drift-flux models are tested at combined low void fractions (between $\sim 10^{-3}$ and $\sim 10^{-1}$) and sub-millimeter bubble sizes, so the determination of drift-flux parameters (distribution parameter, C_0 and drift velocity, U_{gm}) is elaborated. On this account, a bubble size dependent correlation is proposed for U_{gm} determination.

1. Introduction

Gas-liquid two-phase flows are encountered in several engineering applications as well as in the human bloodstream during Decompression Sickness (DCS). DCS is a clinical syndrome caused by the formation of intravascular or extravascular bubbles in the human body as a result of environmental pressure decrease (decompression). Bubbles presence may have mechanical, embolic, and biochemical effects with manifestations ranging from itching and minor pain to neurological symptoms, cardiac failure and death. In current space programs there is a risk of DCS during extravehicular activities, because in that case crewmembers go from a cabin pressure of 14.7 psia (1.0 bar) inside the space shuttle or international space station (ISS) to the space suit pressure of 4.3 psia (0.29 bar). Also, DCS can occur in scuba divers, aviators and compressed air workers [1].

Void fraction is a pivotal dimensionless parameter which is required in the calculation of two-phase mixture density and viscosity, actual phase velocities, pressure drop, heat transfer coefficient, etc. [2]. For this, numerous investigations have been carried out for void fraction measurement (employing e.g. quick closing valve technique, radiation-attenuation method, capacitive sensors, wire-mesh sensors, resistive probes, etc.) and prediction in the past six decades [3–6].

Void fraction in gas-liquid flows depends (apart from the physical properties of the two phases) on several factors including gas/liquid flow rates as well as the relative motion of one phase with respect to the other. In the case of no slip between the two phases (homogeneous flow) combined with uniform void fraction across the pipe, void fraction (α) is equal to the gas volumetric flow fraction (β). The parameter β is defined as the ratio of the gas volumetric flow rate to the total (two-phase mixture) volumetric flow rate or, equally, as the ratio of gas superficial velocity to the total superficial velocity. It is commonly expressed as:

$$\beta = \frac{Q_g}{Q_g + Q_l} = \frac{U_{sg}}{U_{sg} + U_{sl}} \quad (1)$$

where Q_g and Q_l are the gas and liquid volumetric flow rate, respectively, and U_{sg} and U_{sl} are the gas and liquid superficial velocity, respectively [7]. Homogeneous flow can be noticed only in specific bubbly flow applications, since the two phases usually travel with different velocities. In the latter case, void fraction can be predicted employing either a two-fluid model [8] or a drift-flux model [9]. The formulation of a drift-flux model, which is based on the two-phase

* Corresponding author.
E-mail address: karapant@chem.auth.gr (T.D. Karapantsios).

https://doi.org/10.1016/j.expthermflusci.2018.05.018
Received 3 February 2018; Received in revised form 18 May 2018; Accepted 18 May 2018
Available online 22 May 2018
0894-1777/

Nomenclature

α	void fraction
α_{pred}	predicted void fraction based on drift-flux model
α_{exp}	experimental void fraction
β	gas volumetric flow fraction
$\Delta\rho$	density difference between the phases
θ	inclination angle
μ_l	liquid dynamic viscosity
ρ_g	gas density
ρ_l	liquid density
γ	liquid surface tension
C_0	distribution parameter
$C_{0,l}$	distribution parameter for laminar flow
$C_{0,l\rightarrow t}$	distribution parameter for flow transition from laminar to turbulent flow
$C_{0,t}$	distribution parameter for turbulent flow
C_{SDS}	concentration of SDS
D	internal pipe diameter
D^*	dimensionless internal pipe diameter
$D_{1,0}$	arithmetic mean bubble diameter
$D_{3,2}$	surface mean bubble diameter
$D_{4,3}$	volume mean bubble diameter
D_b	bubble diameter
DCS	decompression sickness
D_{Sm}	bubble Sauter mean diameter
g	gravitational acceleration
G	mass flux
Q_g	gas volumetric flow rate
Q_l	liquid volumetric flow rate
Re	Reynolds number of liquid phase
SDS	Sodium Dodecyl Sulfate
U_{sg}	gas superficial velocity
U_{sl}	liquid superficial velocity
U_{gm}	gas phase drift velocity
U_m	two-phase mixture superficial velocity
U_T	bubble rising velocity
x	flow quality

mixture balance equations, is simpler than the two-fluid model which is based on the separate balance equations for each phase. Although a drift-flux model is an approximate formulation in comparison with the more rigorous two-fluid formulation, it is of considerable importance due to its simplicity and applicability to a wide range of two-phase flow problems [10]. Several researchers such as Woldesemayat and Ghajar [11], Godbole et al. [12] and Bhagwat and Ghajar [7] have strongly recommended the use of drift-flux model for vertical upward two-phase flow.

This study investigates the performance of homogeneous flow model as well as well-known drift-flux model based correlations concerning void fraction prediction in a gas-liquid (bubbly) flow that is encountered in human bloodstream during Decompression Sickness [1]. Despite the different local characteristics, similar average bubbly flow conditions are also found in flow boiling in macro-channels [13,14] and other relevant two-phase flow systems. To our knowledge, this is the first time that drift-flux model is examined at such low average void fraction values (between $\sim 10^{-3}$ and $\sim 10^{-1}$) in conjunction to very small bubbles (< 1 mm), as those observed during DCS. Therefore, determination of drift-flux parameters is carefully elaborated in an effort to extend model's capacity to the range of bubble sizes and void fractions examined herein. The next section describes briefly the drift-flux model and outlines the relevant correlations that interest the present study. Predicted void fraction values employing these correlations are compared with experimental data provided in [15,16]. Results are presented and discussed in a following section.

2. Drift-flux model

2.1. Brief description

The drift-flux model, as proposed by Zuber and Findlay [9], assumes that the void fraction occurring in two-phase gas/liquid flows can be attributed to: the radial heterogeneities of void fraction due to transverse forces and the relative velocity between the phases due to axial forces. These effects are taken into account by the distribution parameter, C_0 and the drift velocity, U_{gm}, respectively. The real advantage of drift-flux model lies at its area-averaged form that allows derivation of one-dimensional drift-flux model (Eq. (2)), where α_{pred} represents the void fraction and U_m the two-phase mixture superficial velocity:

$$\langle \alpha_{pred} \rangle = \frac{\langle U_{sg} \rangle}{C_0 \langle U_m \rangle + U_{gm}} \tag{2}$$

The brackets represent area-averaged quantities, but the cross-sectional and volumetric void fraction are equal in the case of non-boiling two phase flow where the cross-sectional distribution of the gas phase with respect to the liquid phase remains virtually unaltered over a short length of the flow. Henceforth, the void fraction is simply expressed as $< \alpha_{pred} > = \alpha_{pred}$. Similar justification is applicable for all cross-sectional averaged quantities involved in Eq. (2) [17].

Therefore, a drift-flux model can be applied to predict the mean void fraction from the known macroscopic quantities U_{sg} and U_{sl} simply by using appropriate models for C_0 and U_{gm}. C_0 is affected by flow pattern, flow channel geometry, flow channel size, flow orientation, pressure, liquid velocity, bubble size, gravitational acceleration and phase change [18]. On the other hand, U_{gm} is influenced by flow pattern, flow channel confinement, and flow channel size. It is mentioned that drift-flux model is valuable when U_{gm} is significantly larger than the total volumetric flux ($U_{gm} > 0.05\ U_m$). For this, it is recommended for dispersed bubbly, bubbly and slug flow patterns [17]. Moreover, the drift-flux equation reduces to the homogeneous flow model when $C_0 = 1$ (implying void fraction homogeneity across the pipe) and $U_{gm} = 0$ (implying no slip between the two phases).

2.2. Correlations for upward bubbly flow

Drift-flux model parameters have been studied extensively in literature for different two-phase flow conditions. In the bubbly flow regime, the gas phase is dispersed in the continuous liquid phase and the flow pattern is symmetrical about the longitudinal flow axis. As initially pointed out by Zuber and Findlay [9], at wall-peaking void fraction conditions the distribution parameter C_0 is expected to be below one, $C_0 < 1$, while for core peaking void fraction conditions $C_0 > 1$. For the bubbly vertical upflow regime, Zuber and Findlay [9] recommended $C_0 = 1.2$. Later, Wallis [19] suggested $C_0 = 1.0$ for the bubbly flow regime with one-dimensional vertical upflow of small, isolated bubbles without coalescence. Both Zuber and Findlay [9] and Wallis [19] determined drift velocity (U_{gm}) by Eq. (3), where γ is the liquid surface tension and ρ_l, ρ_g the densities of the liquid and gas phase, respectively:

$$U_{gm} = 1.53 \left[g\gamma \left(\frac{\rho_l - \rho_g}{\rho_l^2} \right) \right]^{0.25} \tag{3}$$

This expression for U_{gm} can be interpreted as the buoyancy effect that increases the rise velocity of bubbles with respect to homogeneous flow [20]. It must be noted that Eq. (3) refers to bubbles larger than 1.5 mm whose terminal velocity is roughly constant and therefore this model is

independent on bubble size [21].

Bubble size is known to influence strongly the evolution of void fraction radial distribution in upward vertical bubbly flows. In such flows, it has been observed that large bubbles prefer to flow near the center of the pipe whereas small bubbles can be found across the entire cross-section of the pipe, even near the pipe wall. This is related to volume exclusion effects towards the wall, interactions between the wake of bubbles and the velocity distribution of the liquid [22]. C_o should therefore be given as a function of bubble size. Indeed, Hibiki and Ishii [10,23] successfully applied such a bubble size dependent distribution parameter model for finely dispersed bubbly flow in small diameter pipes. According to these authors, in fully developed flows, C_o is defined from Eqs. (4–6) for laminar flow, turbulent flow and flow transition from laminar to turbulent flow, respectively:

$$C_{0,l} = 2-\sqrt{\frac{\rho_g}{\rho_l}} \tag{4}$$

$$C_{0,t} = \left(1.2-0.2\sqrt{\frac{\rho_g}{\rho_l}}\right)\left(1-e^{(-22 < D_{Sm} > /D)}\right) \tag{5}$$

$$C_{0,l\to t} = 2.0e^{(-0.000584\mathrm{Re})} + 1.2\left(1-e^{(-22 < D_{Sm} > /D)}\right)\left(1-e^{(-0.000584\mathrm{Re})}\right)- \left[2.0e^{(-0.000584\mathrm{Re})} + 1.2\left(1-e^{(-22 < D_{Sm} > /D)}\right)\left(1-e^{(-0.000584\mathrm{Re})}\right)-1\right]\sqrt{\frac{\rho_g}{\rho_l}} \tag{6}$$

where D_{Sm} is the bubble Sauter mean diameter $D_{3,2}$, D is the pipe diameter and Re is the Reynolds number (defined by $\rho_l U_{sl} D/\mu_l$, where μ_l is

Table 1
Expressions of thirteen selected drift-flux model based correlations.

Drift-flux model	Definition of parameters
Nicklin et al. [24]	$C_0 = 1.2$ $U_{gm} = 0.35\sqrt{gD}$
Zuber and Findlay [9]	$C_0 = 1.2$ $U_{gm} = 1.53\left[g\gamma\left(\frac{\rho_l-\rho_g}{\rho_l^2}\right)\right]^{0.25}$
Wallis [19]	$C_0 = 1.0$ $U_{gm} = 1.53\left[g\gamma\left(\frac{\rho_l-\rho_g}{\rho_l^2}\right)\right]^{0.25}$
Rouhani and Axelsson [25]	$C_0 = 1.0 + 0.2(1-x)\left(\frac{gD\rho_l^2}{G^2}\right)^{0.25}$ $U_{gm} = 1.18\left[g\gamma\left(\frac{\rho_l-\rho_g}{\rho_l^2}\right)\right]^{0.25}$
Bonnecaze et al. [26]	$C_0 = 1.2$ $U_{gm} = 0.35\sqrt{gD}\left(1-\frac{\rho_g}{\rho_l}\right)$
Greskovich and Cooper [27]	$C_0 = 1.0$ $U_{gm} = 0.671\sqrt{gD}\,(\sin\theta)^{0.263}$
Kokal and Stanislav [28]	$C_0 = 1.2$ $U_{gm} = 0.345\sqrt{gD\left(1-\frac{\rho_g}{\rho_l}\right)}$
Hasan [29]	$C_0 = 1.12$ $U_{gm} = 0.345\sqrt{gD\left(1-\frac{\rho_g}{\rho_l}\right)}$
Gomez et al. [30]	$C_0 = 1.15$ $U_{gm} = 1.53\left[g\gamma\left(\frac{\rho_l-\rho_g}{\rho_l^2}\right)\right]^{0.25}(1-\alpha)^{0.5}\sin\theta$
Hibiki and Ishii [10,23]	$C_{0,l} = 2-\sqrt{\frac{\rho_g}{\rho_l}}$ $C_{0,t} = \left(1.2-0.2\sqrt{\frac{\rho_g}{\rho_l}}\right)\left(1-e^{(-22 < D_{Sm} > /D)}\right)$ $C_{0,l\to t} = 2.0e^{(-0.000584\mathrm{Re})} + 1.2\left(1-e^{(-22 < D_{Sm} > /D)}\right)\left(1-e^{(-0.000584\mathrm{Re})}\right)-$ $\left[2.0e^{(-0.000584\mathrm{Re})} + 1.2\left(1-e^{(-22 < D_{Sm} > /D)}\right)\left(1-e^{(-0.000584\mathrm{Re})}\right)-1\right]\sqrt{\frac{\rho_g}{\rho_l}}$ $U_{gm} = \sqrt{2}\left[g\gamma\left(\frac{\rho_l-\rho_g}{\rho_l^2}\right)\right]^{0.25}(1-\alpha)^{1.75}$
Woldesemayat and Ghajar [11]	$C_0 = \frac{U_{sg}}{U_{sg}+U_{sl}}\left[1+\left(\frac{U_{sl}}{U_{sg}}\right)^{\left(\frac{\rho_g}{\rho_l}\right)^{0.1}}\right]$ $U_{gm} = 2.9(1.22 + 1.22\sin\theta)^{\frac{Patm}{P_{sys}}}\left[\frac{gD\gamma(1+\cos\theta)(\rho_l-\rho_g)}{\rho_l^2}\right]^{0.25}$
Schmidt et al. [31]	$C_0 = aU_m^{-b} + 1$ a = 0.443, b = 0.58 for μ_l = 0.001 Pa·s a = 1.218, b = 0.246 for μ_l = 1-7 Pa·s
Choi et al. [32]	$C_0 = \frac{2}{1+\left(\frac{\mathrm{Re}}{1000}\right)^2} + \frac{1.2-0.2\sqrt{\frac{\rho_g}{\rho_l}}\left(1-e^{-18\alpha}\right)}{1+\left(\frac{1000}{\mathrm{Re}}\right)^2}$ $U_{gm} = 0.0246\cos\theta + 1.606\left[g\gamma\left(\frac{\rho_l-\rho_g}{\rho_l^2}\right)\right]^{0.25}\sin\theta$

the liquid viscosity). The applicability of this model has been confirmed for the experimental conditions: $26 \le U_{sl} \le 500$ cm/s, $U_{sg} \ge 2$ cm/s, $0 \le \alpha \le 0.3$, $25.4 \le D \le 60.0$ mm and 1.40 mm $\le D_{Sm}$. Hibiki and Ishii [10,23] proposed a modified version of Eq. (3) for the determination of drift velocity that incorporates a correlation with void fraction, Eq. (7):

$$U_{gm} = \sqrt{2}\left[g\gamma\left(\frac{\rho_l-\rho_g}{\rho_l^2}\right)\right]^{0.25}(1-\alpha)^{1.75} \quad (7)$$

Because of Eq. (7) the solution of Eq. (2) is not straightforward anymore.

In addition to the two principal correlations for upward bubbly flow [9,19] and the Hibiki and Ishii [10,23] correlation that includes a dependence on bubble size, this study examines the performance of ten other appropriate versions of drift-flux model selected from literature. These ten correlations define drift-flux model parameters C_0 and U_{gm} as shown in Table 1. Seven correlations (Nicklin et al. [24]; Rouhani and Axelsson [25]; Bonnecaze et al. [26]; Greskovich and Cooper [27]; Kokal and Stainslav [28]; Hasan [29]; Gomez et al. [30]) are selected because of their satisfactory performance in upward bubbly flow for D ranging from 12 mm to 50 mm and $\alpha < 0.5$ in air-water/glycerin/kerosene systems, as reported by several researchers (e.g. Bhagwat and Ghajar [7]; Godbole et al. [12]). It is worth-noticing that all correlations, except that of Rouhani and Axelsson [25], suggest C_0 values ranging from 1.0 to 1.2 which are close to the values suggested by Zuber and Findlay [9] and Wallis [19]. On the other hand, the correlations of Woldesemayat and Ghajar [11], Schmidt et al. [31] and Choi et al. [32] are applicable to a wide range of flow conditions due to their flow pattern independent nature. Specifically, the model of Woldesemayat and Ghajar [11] is applicable to natural gas/air-water/kerosene two-phase flows in vertical/horizontal/inclined pipes, for $10 \le D \le 100$ mm. The correlation of Schmidt et al. [31], on the other hand, correlates sufficiently void fraction measurements inside a vertical pipe ($D = 54.5$ mm) for $U_{sl} \le 340$ cm/s, $U_{sg} \le 3000$ cm/s, $1 \le \mu_l \le 7000$ mPa·s, $0.91 \le \rho_g \le 2.29$ kg/m^3 and $982 \le \rho_l \le 1094$ kg/m^3. Furthermore, the applicability of Choi et al. [32] has been confirmed for $50 \le D \le 150$ mm, $0.1 \le U_{sl} \le 100$ cm/s, $10 \le U_{sg} \le 1500$ cm/s, $1 \le \mu_l \le 600$ mPa·s, $2 \le \rho_g \le 4$ kg/m^3, $800 \le \rho_l \le 1000$ kg/m^3. These flow pattern independent models are considered attractive because they correlate both C_0 and U_{gm} with phase velocities and physical properties and furthermore they have described acceptably numerous experimental data.

3. Experimental database

In an effort to evaluate void fraction correlations, both homogeneous flow model and drift-flux model based predictions are compared with 106 experimental data points. These experimental data are presented in [15,16] and concern a vertical co-current upward two-phase (gas-liquid) flow that resembles Decompression Sickness conditions and can be also found in other two-phase flow systems, e.g., flow boiling in macro-channels. Flow loop operation is described in details in Evgenidis and Karapantsios [33]. Void fraction is measured at three axial locations along the flow by means of Electrical Resistance Tomography (ERT) and Differential Pressure (ΔP) inside a pipe with internal diameter $D = 21$ mm. This diameter is equal to the diameter of human vena cava where bubbles gather during a decompression incident [1]. ERT measurements focus on the determination of average void fraction across one plane. Nonetheless, bubbly flow symmetry across the pipe is confirmed for all experimental conditions [34]. Representative ERT images are shown in [33]. ERT and ΔP measurements are in fair agreement, with void fraction being practically equal along the flow [16]. Predicted void fraction values are compared to ΔP experimental data for convenience but also because pressure measurements are more common and so they may allow direct comparison with other works in the future. Liquid superficial velocity (U_{sl}) values range from ~3 to ~30 cm/s, as these values are representative of the bloodstream in human vena cava. On the other hand, gas superficial velocity (U_{sg}) values range from ~0.05 to ~1.2 cm/s providing average void fraction values between $\sim 10^{-3}$ and $\sim 10^{-1}$ which represent Decompression Sickness incidents with potential pathological effects. Experiments are performed at 37 °C, same as the body temperature, with two different test liquids: **(a)** An aqueous solution of NaCl (0.02% w/w), henceforth called ***Water*** and **(b)** An aqueous solution of glycerol (56.0% w/w) and NaCl (1.3% w/w), henceforth called ***Blood***, simulating human blood physical properties. Since the physical properties of the applied test liquids have been already presented in [16] and [33], they can be found here in Supplementary Table 1. Helium gas is chosen for bubbles production due to its low solubility in the test liquids, while bubble size is varied using prescribed surfactant (SDS) concentrations: 5 and 500 ppm in *Water*; 0 and 500 ppm in *Blood*. These two concentrations provide fairly distinct Bubble Size Distributions (BSDs) for each test liquid, while average bubble size is always below 1 mm. BSDs are measured for each experimental run applying an optical method (Evgenidis et al. [35]).

4. Results and discussion

4.1. Correlation of void fraction measurements with drift-flux model in Water

First, it is investigated whether experimental data from Evgenidis [15] and Evgenidis and Karapantsios [16] conform to the homogeneous flow model, Eq. (1), which is a sub-case of the drift-flux model, Eq. (2), when $C_0 = 1$ and $U_{gm} = 0$. Fig. 1 compares the experimental void fraction α_{exp} with the estimated gas volumetric fraction of the homogeneous flow model, β (Eq. (1)), for the examined range of U_{sl}, U_{sg} and C_{SDS} in *Water*. Error bars indicating standard deviation values from repeated runs have been added to experimental void fraction data; in most cases error bars are smaller than data markers. The addition of 5 ppm SDS yields arithmetic mean bubble diameters $D_{1,0}$ ranging from 200 to 800 μm, while addition of 500 ppm SDS gives $D_{1,0}$ in the range 50–100 μm. Due to the different bubble sizes, similar U_{sl} and U_{sg} values provide different void fraction values at the two SDS concentrations. It is apparent that the homogeneous flow model predictions cannot correlate favorably with all experimental data. The goodness of correlation between experimental and predicted void fractions is expressed by the Mean Absolute Percentage Error (MAPE). For $C_{SDS} = 500$ ppm, the

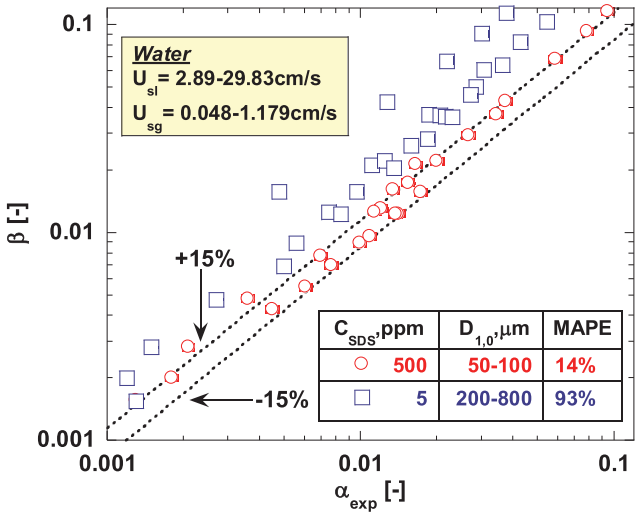

Fig. 1. Comparison of experimentally measured void fraction (α_{exp}) with estimated gas volumetric flow fraction from homogeneous flow model (β), for $C_{SDS} = 5$ ppm ($D_{1,0}$: 200–800 μm) and $C_{SDS} = 500$ ppm ($D_{1,0}$: 50–100 μm) in *Water*.

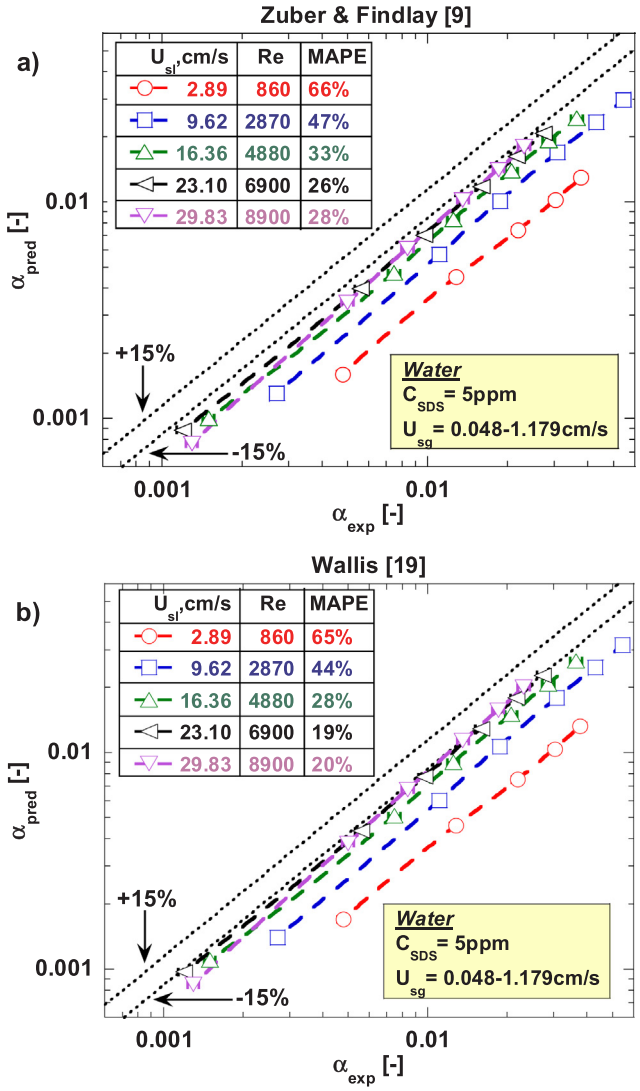

Fig. 2. Comparison of experimentally measured void fraction (α_{exp}) with estimated void fraction by **(a)** Zuber and Findlay [9] and **(b)** Wallis [19] drift-flux models, for C_{SDS} = 5 ppm in *Water*.

Table 2
Mean Absolute Percentage Error (MAPE, %) values for varying superficial liquid velocities (U_{sl}) employing nine selected drift-flux model based correlations for C_{SDS} = 5 ppm in *Water*.

Drift-flux model	U_{sl}, cm/s					Mean Absolute Percentage Error (MAPE), %
	2.89	9.62	16.36	23.10	29.83	
Nicklin et al. [24]	51%	31%	18%	12%	17%	
Rouhani and Axelsson [25]	60%	42%	28%	21%	23%	
Bonnecaze et al. [26]	51%	31%	18%	12%	17%	
Greskovich and Cooper [27]	71%	52%	37%	28%	28%	
Kokal and Stainslav [28]	50%	30%	17%	12%	16%	
Hasan [29]	49%	28%	14%	08%	12%	
Gomez et al. [30]	65%	46%	32%	25%	26%	
Woldesemayat and Ghajar [11]	78%	57%	35%	16%	06%	
Choi et al. [32]	67%	48%	34%	27%	29%	

homogeneous flow model predicts void fraction within reasonable (± 15%) error bands of the experimental data (MAPE: 14%). This indicates that void fraction is quite uniform at the pipe cross-section and that bubbles travel approximately with the velocity of the liquid. On the contrary, estimations of the homogeneous model overpredict the experimental void fraction for C_{SDS} = 5 ppm (MAPE: 93%) where bubbles

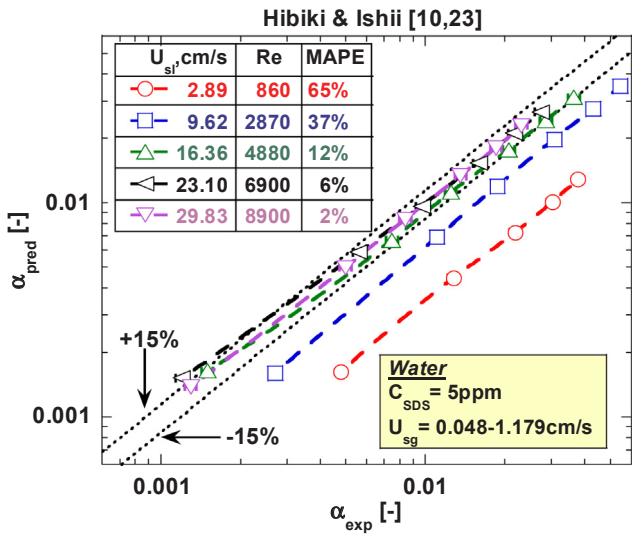

Fig. 3. Comparison of experimentally measured void fraction (α_{exp}) with estimated void fraction by Hibiki and Ishii [10,23] drift-flux model for C_{SDS} = 5 ppm in *Water*.

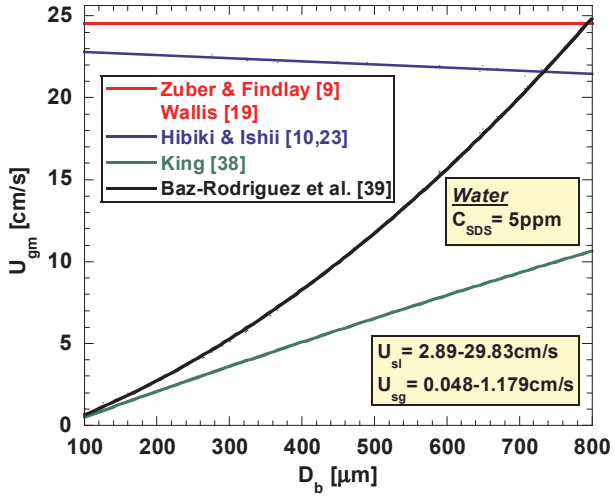

Fig. 4. Estimated drift velocity (U_{gm}) as a function of average bubble diameter (D_b) for C_{SDS} = 5 ppm in *Water*, using bubble size dependent (King [38]; Baz-Rodriguez et al. [39]) and non-dependent (Zuber and Findlay [9]; Wallis [19]; Hibiki and Ishii [10,23]) models.

are larger than for C_{SDS} = 500 ppm. This suggests a core peaking void fraction profile (C_0 > 1) or/and a non-zero drift velocity of bubbles (U_{gm} > 0).

Then, the two principal drift-flux model based equations, Zuber and Findlay [9] and Wallis [19], for upward bubbly flow in vertical pipe are tested for C_{SDS} = 5 ppm in Fig. 2a and b. Zuber and Findlay [9] and Wallis [19] suggest C_0 = 1.2 and C_0 = 1.0 in Eq. (2), respectively, with U_{gm} estimated by Eq. (3) in both models. It is shown that these models overall do not succeed in correlating experimental data for C_{SDS} = 5 ppm in *Water*. Contrary to the homogeneous flow model, Zuber and Findlay [9] and Wallis [19] models underpredict void fraction. Since both models use C_0 values around 1, the discrepancy may be chiefly attributed to U_{gm} overestimation from Eq. (3) that actually concerns bubbles larger than 1.5 mm where buoyancy effect is higher. As U_{sl} and consequently U_m increases, the contribution of U_{gm} in void fraction estimation decreases (Eq. (2)) and thus the deviation between experimental and theoretical values becomes smaller as shown by MAPE values in Fig. 2a and b. This observation is further supported by employing the selected drift-flux model correlations of Table 1, except

Table 3
Mean Absolute Percentage Error (MAPE, %) values for varying superficial liquid velocities (U_{sl}) employing thirteen drift-flux model based correlations for C_0 determination and King [38] model for U_{gm} determination, for C_{SDS} = 5 ppm in *Water*.

Drift-flux model	U_{sl}, cm/s					Mean Absolute Percentage Error (MAPE), %
	2.89	9.62	16.36	23.10	29.83	
Nicklin et al. [24]	10%	11%	11%	07%	11%	
Zuber and Findlay [9]	10%	11%	11%	07%	11%	
Wallis [19]	10%	08%	12%	13%	02%	
Rouhani and Axelsson [25]	19%	18%	14%	10%	13%	
Bonnecaze et al. [26]	10%	11%	11%	07%	11%	
Greskovich and Cooper [27]	10%	08%	12%	13%	02%	
Kokal and Stainslav [28]	10%	11%	11%	07%	11%	
Hasan [29]	10%	09%	10%	06%	06%	
Gomez et al. [30]	10%	09%	10%	06%	08%	
Hibiki and Ishii [10,23]	23%	16%	55%	62%	38%	
Woldesemayat and Ghajar [11]	37%	89%	>100%	>100%	>100%	
Schmidt et al. [31] for μ_l = 0.001 Pa.s	10%	08%	11%	07%	03%	
Choi et al. [32]	16%	12%	12%	08%	11%	

Schmidt et al. [31] that provides only C_0 correlation and not U_{gm} correlation and Hibiki and Ishii [10,23] which is examined separately afterwards. It is reminded that six of them suggest also C_0 values between 1.0 and 1.2. Table 2 presents the deviation of experimental and predicted void fractions by means of MAPE values for all the examined models. Apparently, MAPE values decrease considerably when U_{sl} increases, as already noticed with the two principal correlations of Zuber and Findlay [9] and Wallis [19]. Although four models (Nicklin et al. [24]; Bonnecaze et al. [26]; Kokal and Stainslav [28]; Hasan [29]) yield fair MAPE values (< 20%) for U_{sl} > 16.36 cm/s, it is crucial to investigate whether the agreement can be improved and also extended to a broader range of conditions within those examined in the present study.

Hibiki and Ishii [10,23] model is tested separately (Fig. 3), since it has been strongly recommended for the current bubbly flow conditions due to the small dimensionless diameter of the pipe ($D^* = D/\sqrt{\sigma/g\Delta\rho}$), i.e., 8.5 (Schlegel et al. [36]). These researchers suggested a bubble size dependent C_0 parameter and, furthermore, correlated U_{gm} with void fraction, Eq. (7). C_0 is calculated employing Eqs. (4–6) for U_{sl} = 2.89 cm/s (Re = 860, laminar flow), U_{sl} = 9.62 cm/s (Re = 2870, transition from laminar to turbulent flow) and U_{sl} = 16.36, 23.10, 29.83 cm/s (Re = 4880, 6900, 8900, turbulent flow), respectively. The present D_{Sm} values used as input for C_0 determination through Eqs. (5) and (6) have been estimated by optical measurements and range from 300 to 1200 μm. Fig. 3 manifests that the estimated void fraction values approach the measured ones as U_{sl} increases. As a matter of fact, Hibiki and Ishii [10,23] model predicts void fraction within the ± 15% error bands of the experimental data for the three highest examined U_{sl} values (16.36, 23.10, 29.83 cm/s). The corresponding MAPE values are considered pretty satisfactory: 12%, 6% and 2%. Therefore, one might argue that the applicability of this model extends down to (i) U_{sl} = 16 cm/s (originally proposed $U_{sl} \geq$ 26 cm/s), (ii) U_{sg} = 0.05 cm/s (originally proposed $U_{sg} \geq$ 2 cm/s), (iii) D = 21 mm (originally proposed $D \geq$ 25.4 mm) and (iv) D_{Sm} = 300 μm (originally proposed $D_{Sm} \geq$ 1.40 mm).

In view of the failure of the aforementioned drift-flux models to correlate successfully allthepresent data for C_{SDS} = 5 ppm, an effort is made to check if other U_{gm} values can be defined that may be more suitable to do the work. In the above models, U_{gm} is determined by equations that do not include any dependence on bubble size. However, the latter is rather the case for sub-millimeter bubbles (Rodrigue [37]).

In this respect, Fig. 4 compares the U_{gm} predictions of Zuber and Findlay [9], Wallis [19] and Hibiki and Ishii [10,23] models with the predictions of the models of King [38] and Baz-Rodriguez et al. [39] in which U_{gm} depends largely on bubble size. Predictions are shown as a function of mean bubble diameter covering the range encountered in *Water* with C_{SDS} = 5 ppm. It is reminded that predictions of Zuber and Findlay [9] and Wallis [19] are based on Eq. (3), while predictions of Hibiki and Ishii [10,23] are based on Eq. (7) including a correlation with void fraction. On the other hand, King [38] defines the rising velocity (U_T) of fully dispersed swarm of spherical bubbles of *identical* size in a *contaminated* liquid by Eq. (8), where D_b is the bubble diameter:

$$U_T = \left(\frac{4gD_b}{3C}\right)^{1/2} \tag{8}$$

where:

$$C = 0.28\left(\frac{(1 + 0.0921f^{1/2})^{1/2} + 1}{(1 + 0.0921f^{1/2})^{1/2} - 1}\right)^2 \tag{9}$$

and:

$$f = \frac{4}{3}gD_b^3\left(\frac{\rho_l}{\mu_l}\right)^2 \tag{10}$$

Contrary to King [38], Baz-Rodriguez et al. [39] refer to *single* spherical bubbles rising in *pure* liquids. They propose the following formulation for U_T:

$$U_T \frac{1}{\sqrt{\frac{1}{U_{T1}^2} + \frac{1}{U_{T2}^2}}} \tag{11}$$

where U_{T1} (Eq. (12)) is the rise velocity when viscous effects are important and U_{T2} (Eq. (14)) is the corresponding velocity when surface tension effects are significant:

$$U_{T1} = U_{Tpot}\left[1 + 0.73667\frac{(gD_b)^{1/2}}{U_{Tpot}}\right]^{1/2} \tag{12}$$

where:

$$U_{Tpot} = \frac{1}{36}\frac{\Delta\rho g D_b}{\mu_l} \tag{13}$$

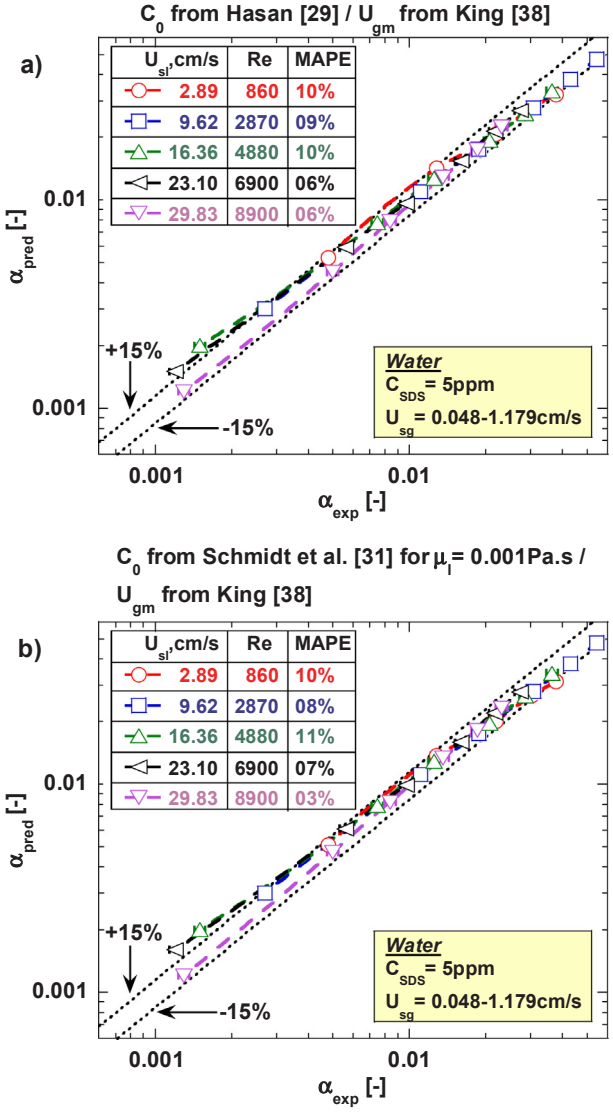

Fig. 5. Comparison of experimentally measured void fraction (α_{exp}) with estimated void fraction applying **(a)** Hasan [29] and **(b)** Schmidt et al. [31] for μ_l = 0.001 Pa·s drift-flux models regarding C_0 determination and King [38] concerning U_{gm} determination, for C_{SDS} = 5 ppm in *Water*.

and:

$$U_{T2} = \left(\frac{3\gamma}{\rho_l D_b} + \frac{gD_b(\rho_l - \rho_g)}{2\rho_l} \right) \quad (14)$$

Finally, U_{gm} values are computed by subtracting U_{sg} from U_T values estimated either by King [38] or Baz-Rodriguez et al. [39] model.

Fig. 4 shows that Zuber and Findlay [9] and Wallis [19] provide a constant U_{gm} value for C_{SDS} = 5 ppm. U_{gm} values computed by Hibiki and Ishii [10,23] slightly decrease with increasing average bubble diameter due to the void fraction term effect. On the other hand, U_{gm} values resulting from the bubble size dependent models start from a very low value but increase considerably with bubble size. Baz-Rodriguez et al. [39] model provides higher U_{gm} values than King [38] because it refers to single bubble motion and it does not take into account the interactions with the adjacent bubbles as King [38] does. For this, King [38] model is considered as the most suitable to determine U_{gm} values in the present study. Then, a question arises about the calculation of the proper mean bubble diameter to be used in Eqs. (8) and (10). Volume mean bubble diameter ($D_{4,3}$) is considered more representative from a hydrodynamic point of view in comparison to

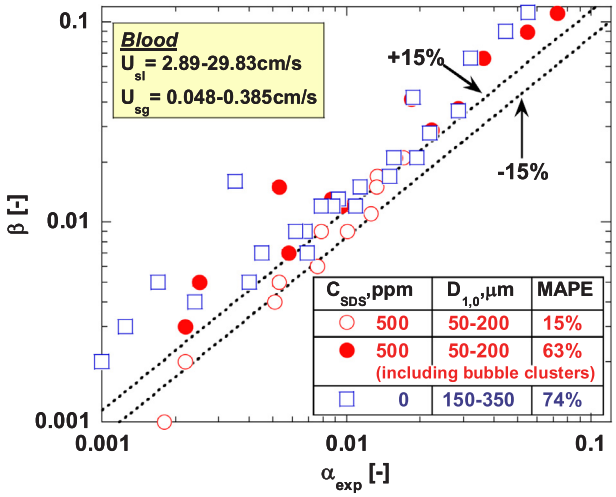

Fig. 6. Comparison of experimentally measured void fraction (α_{exp}) with estimated gas volumetric flow fraction from homogeneous flow model (β), for C_{SDS} = 0 ppm ($D_{1,0}$: 150–350 μm) and C_{SDS} = 500 ppm ($D_{1,0}$: 50–200 μm) in *Blood*.

arithmetic mean diameter ($D_{1,0}$) or surface mean diameter ($D_{3,2}$). Thus, the $D_{4,3}$ diameter is used as an input to King [38] model for the determination of U_{gm}. In any case, the influence of the different mean bubble diameters on drift velocity will be thoroughly investigated in a future work.

Based on the above, experimentally measured void fractions for C_{SDS} = 5 ppm in *Water* are compared to predicted void fraction when C_0 is determined applying thirteen different drift-flux model based equations (listed in Table 1) and U_{gm} is determined by the King [38] model. In this respect, Table 3 summarizes the goodness of correlation between experimental and predicted void fractions by means of MAPE values for varying drift-flux models and liquid superficial velocities. It is seen that most drift-flux models succeed in predicting void fraction within ± 10% of the experimental data. This holds for all U_{sl} values including both laminar and turbulent flow, with *Re* ranging from 860 to 8900. Interestingly, these models apply C_0 values ranging from 1.0 to 1.2. Among them, Hasan [29] and Schmidt et al. [31] for μ_l = 0.001 Pa·s are found to be the top performing. Fig. 5 displays the correlation of the latter two drift-flux models with experimental data, when U_{gm} is determined from King [38] model. MAPE values decrease from ~10% to ~5% with increasing liquid superficial velocity and, consequently, void fraction prediction is considered overall satisfactory. On the contrary, Hibiki and Ishii [10,23] model as well as Woldesemayat and Ghajar [11] model fail to correlate adequately the experimental data. Especially for U_{sl} ranging from 16.36 to 29.83 cm/s (turbulent flow), the performance of Hibiki and Ishii [10,23] model is worse when U_{gm} is determined by the King [38] model (Eq. (8)) than by employing Eq. (5). The performance of Woldesemayat and Ghajar [11], on the other hand, deteriorates when using King [38] model for all examined U_{sl} values (both laminar and turbulent flow). In these conditions, both models apply pretty low and rather erroneous C_0 values (Woldesemayat and Ghajar [11]: down to 0.1, Hibiki and Ishii [10,23]: down to 0.4). Consequently, the better -still poor- performance of pure Hibiki and Ishii [10,23] and Woldesemayat and Ghajar [11] models in these conditions is circumstantial because the error in the determination of C_0 counterbalances the error in the determination of U_{gm}.

Therefore, it may be argued that for the case of C_{SDS} = 5 ppm in *Water*:

(a) Void fraction is roughly uniform at the pipe cross-section since all drift-flux models that correlate successfully experimental data either suggest (e.g. Hasan [29]; Gomez et al. [30]) or estimate (e.g.

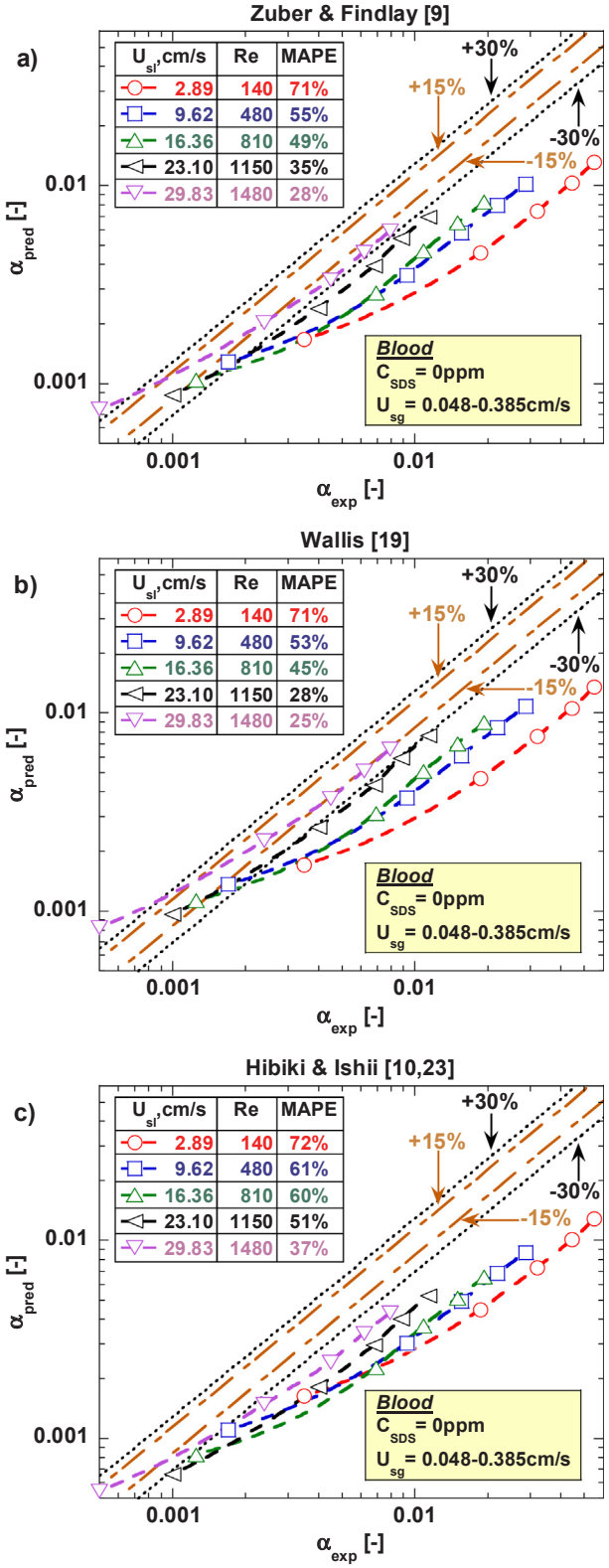

Fig. 7. Comparison of experimentally measured void fraction (α_{exp}) with estimated void fraction by **(a)** Zuber and Findlay [9], **(b)** Wallis [19] and **(c)** Hibiki and Ishii [10,23] drift-flux models, for C_{SDS} = 0 ppm in *Blood*.

Schmidt et al. [31]; Choi et al. [32]) C_0 values ranging from 1.0 to 1.2.

(b) King [38] model succeeds in estimating U_{gm} based on the volume average bubble diameter, $D_{4,3}$.

Table 4
Mean Absolute Percentage Error (MAPE,%) values for varying superficial liquid velocities (U_{sl}) employing nine selected drift-flux model based correlations for C_{SDS} = 0 ppm in *Blood*.

Drift-flux model	U_{sl}, cm/s					Mean Absolute Percentage Error (MAPE), %
	2.89	9.62	16.36	23.10	29.83	
Nicklin et al. [24]	60%	43%	39%	24%	23%	
Rouhani and Axelsson [25]	67%	51%	45%	30%	26%	
Bonnecaze et al. [26]	60%	43%	39%	24%	23%	
Greskovich and Cooper [27]	77%	61%	53%	37%	28%	
Kokal and Stainslav [28]	60%	42%	39%	24%	23%	
Hasan [29]	59%	41%	38%	22%	23%	
Gomez et al. [30]	71%	55%	48%	33%	28%	
Woldesemayat and Ghajar [11]	82%	63%	48%	24%	29%	
Choi et al. [32]	74%	62%	57%	43%	31%	

4.2. Correlation of void fraction measurements with drift-flux model in *Blood*

Void fraction prediction in *Blood* is more complicated. Liquid viscosity is 5 times higher compared to *Water*, while the amount of NaCl added to simulate blood electrical properties is high enough to decrease considerably bubble size (bubble coalescence is hindered by the repulsion of Na^+ adsorbed at interfaces) even in the absence of surface active agent. In addition, the presence of surfactant along with the finite salinity and viscosity of *Blood* results in the formation of several stable bubble clusters that rise inside the pipe among numerous other isolated bubbles, as described in [15,16].

Similarly to Fig. 1 in *Water*, Fig. 6 examines whether the homogeneous flow model correlates satisfactorily the experimental data in *Blood*. In this respect, experimental void fraction measured in both the absence (C_{SDS} = 0 ppm) and the presence of surfactant (C_{SDS} = 500 ppm) is compared to the predicted void fraction applying the homogeneous flow model (Eq. (1)). Addition of SDS decreases $D_{1,0}$ from 150 to 350 μm (C_{SDS} = 0 ppm) to 50–200 μm (C_{SDS} = 500 ppm) despite the formation of bubble clusters in the latter case (clusters are not so many to affect $D_{1,0}$). To separate the effect of bubble clusters on the correlation between measured and theoretical void fraction, experimental data for C_{SDS} = 500 ppm that include bubble clusters are denoted with distinct symbols in Fig. 6. It is seen that the homogeneous flow model predicts void fraction with reasonable accuracy (± 15%) only for those cases with C_{SDS} = 500 ppm where no bubble clusters are noticed. The absence of clusters implies void fraction homogeneity across the pipe ($C_0 \sim 1$) and no slip between the two phases ($U_{gm} \sim 0$). On the other hand, the homogeneous flow model overestimates void fraction for C_{SDS} = 500 ppm in the presence of bubble clusters where the overall MAPE reaches 63%. Although the number of bubble clusters is small to change considerably $D_{1,0}$, however their presence makes the homogeneous flow model to fail in predicting accurately void fraction due to induced C_0 rise (core peaking void fraction profile) or/and non-zero average U_{gm}. Overprediction of experimental void fraction is also noticed for C_{SDS} = 0 ppm (MAPE: 74%) where bubbles are noticeably larger than for C_{SDS} = 500 ppm. The aforementioned findings in *Blood* are qualitatively comparable with those in *Water*.

In the previous section, twelve drift-flux models were found to fail to provide acceptable predictions for all void fraction data for C_{SDS} = 5 ppm in *Water*. This was attributed to U_{gm} overestimation of the bubble sizes actually encountered in this study. Application of the same correlations for C_{SDS} = 0 ppm in *Blood* confirms this finding. Fig. 7**a–c** compare experimental void fraction with the predictions of Zuber and Findlay [9], Wallis [19] and Hibiki and Ishii [10,23] models, respectively. In most cases, the models underestimate significantly the measured void fraction. Moreover, predictions vary non-linearly at the lower void fraction regime (low U_{sg} values). MAPE values decrease from ~70% to ~30% with increasing liquid superficial velocity due to the decreasing U_{gm} contribution in void fraction estimation (Eq. (2)). The

Table 5
Mean Absolute Percentage Error (MAPE, %) values for varying superficial liquid velocities (U_{sl}) employing thirteen drift-flux model based correlations for C_0 determination and King [38] model for U_{gm} determination, for C_{SDS} = 0 ppm in *Blood*.

Drift-flux model	U_{sl}, cm/s					Mean Absolute Percentage Error (MAPE), %
	2.89	9.62	16.36	23.10	29.83	
Nicklin et al. [24]	56%	26%	25%	17%	47%	
Zuber and Findlay [9]	56%	26%	25%	17%	47%	
Wallis [19]	78%	45%	25%	40%	75%	
Rouhani and Axelsson [25]	28%	28%	28%	11%	42%	
Bonnecaze et al. [26]	56%	26%	25%	17%	47%	
Greskovich and Cooper [27]	78%	45%	25%	40%	75%	
Kokal and Stainslav [28]	56%	26%	25%	17%	47%	
Hasan [29]	64%	31%	23%	25%	57%	
Gomez et al. [30]	61%	29%	24%	22%	53%	
Hibiki and Ishii [10,23]	31%	37%	38%	29%	29%	
Woldesemayat and Ghajar [11]	>100%	>100%	>100%	>100%	>100%	
Schmidt et al. [31] for μ_l = 0.001 Pa.s	53%	31%	22%	31%	66%	
Schmidt et al. [31] for μ_l = 1-7 Pa.s	30%	33%	33%	18%	23%	
Choi et al. [32]	31%	35%	34%	17%	23%	

performance of these three models is comparable to each other, although the applied C_0 values differ considerably (from 1 to ~2) while the estimated U_{gm} values hardly varies (from 22 to 24 cm/s). This implies that U_{gm} estimation is erroneous and makes its accurate determination crucial. Table 4 summarizes MAPE values from the comparison of experimental and predicted void fractions based on the nine remaining drift-flux models of Table 1, except Schmidt et al. [31] that provides only C_0 correlation and not U_{gm} correlation. It is clear that no model succeeds in correlating experimental data with a reasonable accuracy for C_{SDS} = 0 ppm in *Blood*, while MAPE values are akin to those for the three models examined previously.

Then, it is investigated whether U_{gm} determination using King [38] improves void fraction prediction for C_{SDS} = 0 ppm in *Blood*, as already shown for C_{SDS} = 5 ppm in *Water*. It is stressed that King [38] model includes a dependence of bubbles rise velocity not only on bubble size but also on liquid viscosity. Thus, it is considered attractive for proper estimation of drift velocity in *Blood,* too. To this end, experimental void fraction is compared with the estimated void fraction applying thirteen drift-flux models for C_0 determination and King [38] model for U_{gm} estimation. The resulting MAPE values for varying U_{sl} values are displayed in Table 5. It is shown that most of the models improve their performance concerning void fraction prediction for C_{SDS} = 0 ppm in *Blood*. Specifically, the performance of two models (Wallis [19], Woldesemayat and Ghajar [11]) deteriorates, while ten models (Nicklin et al. [24], Zuber and Findlay [9], Rouhani and Axelsson [25], Bonnecaze et al. [26], Greskovich and Cooper [27], Kokal and Stainslav [28], Hasan [29], Gomez et al. [30], Hibiki and Ishii [10,23], Choi et al. [32]) perform better. The latter ten models predict 60–100% of experimental data with greater accuracy when employing King [38] for U_{gm} determination. It must be noted that Schmidt et al. [31] does not provide U_{gm} correlation for comparison. Poor performance of Woldesemayat and Ghajar [11] model has been already explained for C_{SDS} = 5 ppm in *Water*, while the failure of Wallis [19] excludes the case of pretty uniform void fraction distribution across the pipe for C_{SDS} = 0 ppm in *Blood*. It is worthy to mention that Hibiki and Ishii [10,23] model performs better using King [38] for U_{gm} estimation, for all examined U_{sl} values (2.89–29.83 cm/s, corresponding to laminar flow where C_0 is set to 2).

Of greater significance is the fact that Rouhani and Axelsson [25], Schmidt et al. [31] for μ_l = 1–7 Pa·s and Choi et al. [32] give satisfactory predictions for C_{SDS} = 0 ppm in *Blood*. Fig. 8a–c display these correlations versus experimental data. It is shown that these three models predict the majority of experimental void fraction data within ± 30%. This performance is considered adequate according to the criterion proposed by Bhagwat & Ghajar [7] that assumes a drift-flux correlation satisfactory if at least 80% of the examined data points are predicted within ± 30%. Yet, the non-linear deviations at low void fractions (low U_{sg} values) still hold. Interestingly, the three top performing correlations for C_{SDS} = 0 ppm in *Blood* do not employ a specific fixed C_0 value, as noticed for C_{SDS} = 5 ppm in *Water* (C_0: 1.0–1.2, indicating roughly uniform void fraction profile across the pipe). They correlate the distribution parameter with phase velocities, liquid physical properties and two-phase flow quality. Increase of U_{sl} from ~3 cm/s to ~30 cm/s (*Re*: 140–1480, all laminar flows) for C_{SDS} = 0 ppm in *Blood* results in decrease of the estimated C_0 values from 1.80 to 1.25 applying Rouhani and Axelsson [25] model, from 1.93 to 1.52 applying Schmidt et al. [31] model for μ_l = 1–7 Pa·s and from 1.98 to 1.43 applying Choi et al. [32] model. This implies a core-peaking void fraction profile which flattens as U_{sl} increases.

5. Conclusions

This work examines the performance of drift-flux model in a gas-liquid flow that is encountered in human bloodstream during Decompression Sickness and additionally found in other two-phase flow applications, e.g., flow boiling in macro-channels. To our knowledge, it is the first time that this model is tested at combined low void fractions (between $\sim 10^{-3}$ and $\sim 10^{-1}$) and sub-millimeter bubble sizes. Predicted void fraction values are compared to experimental data measured in co-current upward bubbly flow for varying gas/liquid flow properties. Water and blood simulant are used as test liquids. Homogeneous flow model (sub-case of drift-flux model) predicts void fraction with an accuracy of ± 15% in water when the mean bubble diameter ranges from 50 to 100 μm as well as in blood simulant for a mean bubble size ranging from 50 to 200 μm. For larger bubbles in water (average size up to 800 μm), thirteen drift-flux models are examined. Among them, only Hibiki and Ishii [10,23] predicts satisfactorily a part of void fraction data and this failure is attributed to the determination of drift velocity by expressions that do not include a dependence on bubble size. When a bubble size dependent model (King

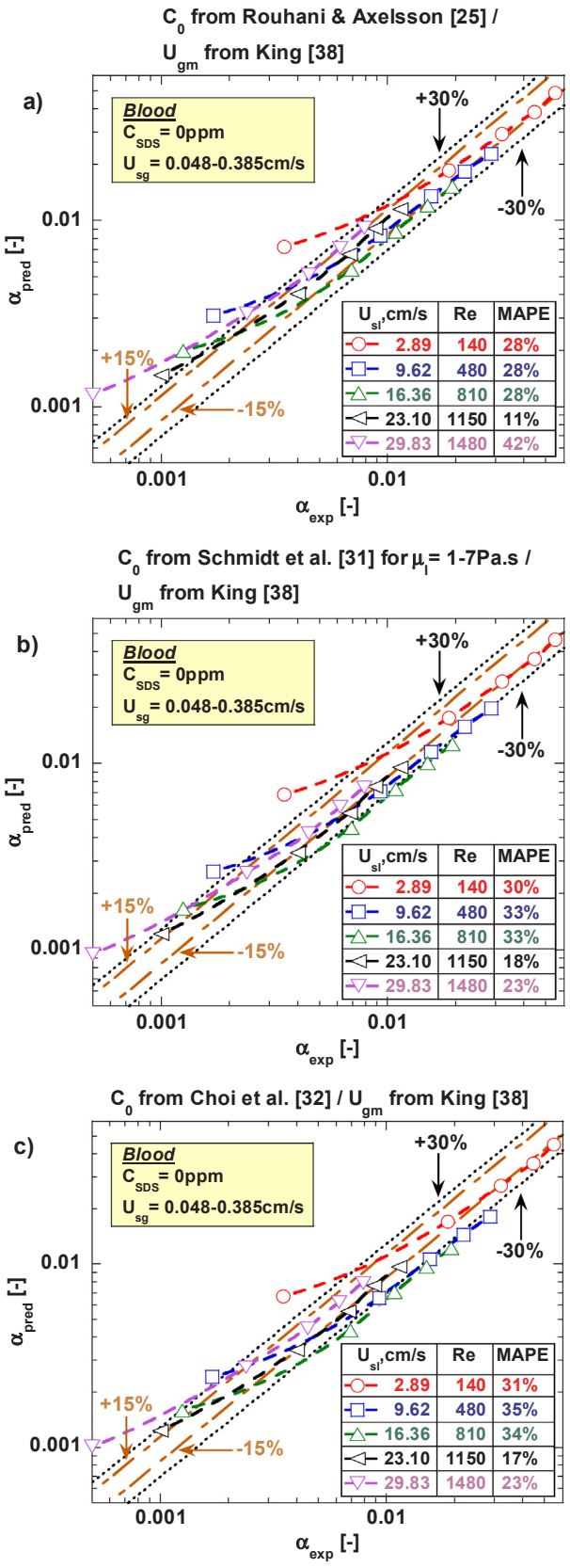

Fig. 8. Comparison of experimentally measured void fraction (α_{exp}) with estimated void fraction applying **(a)** Rouhani and Axelsson [25], **(b)** Schmidt et al. [31] for μ_l = 1–7 Pa·s and **(c)** Choi et al. [32] drift-flux models regarding C_o determination and King [38] concerning U_{gm} determination, for C_{SDS} = 0 ppm in *Blood*.

[38]) is used for estimating drift velocity, the performance of eleven drift-flux models, suggesting roughly uniform void fraction across the pipe, improves substantially and correlate experimental data with an accuracy of ± 10%. In blood simulant, for mean bubble sizes up to 350 μm, three drift-flux models, suggesting core-peaking void fraction conditions, succeed to correlate satisfactorily experimental data (80% of data points predicted within ± 30%), applying King [38] model. Even so, a non-linear deviation of predictions from measurements still exists at low void fractions (low superficial gas velocities).

Acknowledgements

This study was funded by esa (GSTP Project: In-Vivo Embolic Detector, I-VED - Contract No.: 4000101764 and MAP Project: Convective boiling and condensation local analysis and modelling of dynamics and transfers, MANBO – Contract No.: 4200020289) and carried out under the umbrella of COST Action MP1106: 'Smart and green interfaces—from single bubbles and drops to industrial, environmental and biomedical applications' and COST Action MP1305: 'Flowing Matter'. The view expressed herein can in no way be taken to reflect the official opinion of the European Space Agency.

Appendix A. Supplementary material

Supplementary data associated with this article can be found, in the online version, at http://dx.doi.org/10.1016/j.expthermflusci.2018.05.018.

References

[1] R.D. Vann, F.K. Butler, S.J. Mitchell, R.E. Moon, Decompression illness, The Lancet 377 (2011) 153–164.
[2] S.M. Bhagwat, A.J. Ghajar, Experimental investigation of non-boiling gas-liquid two phase flow in downward inclined pipes, Exp. Therm. Fluid Sci. 89 (2017) 219–237.
[3] F.T. Kazinawa, G. Ribatski, Void fraction and pressure drop during external upward two-phase crossflow in tube bundles – part I: Experimental investigation, Int. J. Heat Fluid Fl. 65 (2017) 200–209.
[4] F.T. Kazinawa, G. Ribatski, Void fraction and pressure drop during external upward two-phase crossflow in tube bundles – part II: Predictive methods, Int. J. Heat Fluid Fl. 65 (2017) 210–219.
[5] R. Kurimoto, K. Nakazawa, H. Minagawa, T. Yasuda, Prediction models of void fraction and pressure drop for gas-liquid slug flow in microchannels, Exp. Therm. Fluid Sci. 88 (2017) 124–133.
[6] S.M. Salehi, H. Karimi, R. Moosavi, A.A. Dastranj, Different configurations of capacitance sensor for gas/oil two phase flow measurement: An experimental and numerical study, Exp. Therm. Fluid Sci. 82 (2017) 349–358.
[7] S.M. Bhagwat, A.J. Ghajar, Similarities and differences in the flow patterns and void fraction in vertical upward and downward two phase flow, Exp. Therm. Fluid Sci. 39 (2012) 231 227.
[8] J.M. Delhaye, Equations fondamentales des écoulements diphasiques, Part 1 and 2, CEA-R-3429, France, 1968.
[9] N. Zuber, J.A. Findlay, Average volumetric concentration in two-phase flow systems, J. Heat Transfer 87 (1965) 453–468.
[10] T. Hibiki, M. Ishii, Distribution parameter and drift velocity of drift-flux model in bubbly flow, Int. J. Heat Mass Tran. 45 (2002) 707–721.
[11] M.A. Woldesemayat, A.J. Ghajar, Comparison of void fraction correlations for different flow patterns in horizontal and upward inclined pipes, Int. J. Multiphas. Flow 33 (4) (2007) 347–370.
[12] P.V. Godbole, C.G. Tang, A.J. Ghajar, Comparison of void fraction correlations for different flow patterns in upward vertical two-phase flow, Heat Transfer Eng. 32 (10) (2011) 843–860.
[13] R. Maurus, V. Ilchenko, T. Sattelmayer, Study of the bubble characteristics and the local void fraction in subcooled flow boiling using digital imaging and analyzing techniques, Exp. Therm. Fluid. Sci. 26 (2002) 147–155.
[14] J. Yoo, C.E. Estrada-Perez, Y.A. Hassan, Experimental study on bubble dynamics and wall heat transfer arising from a single nucleation site at subcooled flow boiling conditions – Part 1: experimental methods and data quality verification, Int. J. Multiph. Flow 84 (2016) 315–324.
[15] S.P. Evgenidis, Development of an electrical technique for detection and characterization of bubbles in liquid flows, PhD Thesis Aristotle University of Thessaloniki, Greece, 2011.
[16] S. Evgenidis, T. Karapantsios, Gas-liquid flow of sub-millimeter bubbles at low void fractions: experimental study of bubble size distribution and void fraction, Int. J. Heat Fluid Fl. 71 (2018) 353–365.
[17] S.M. Bhagwat, A.J. Ghajar, A flow pattern independent drift flux model based void fraction correlation for a wide range of gas-liquid two phase flow, Int. J. Multiphas.

Flow 59 (2014) 186–205.
[18] T. Ozaki, T. Hibiki, Drift-flux model for rod bundle geometry, Pro. Nucl. Energ. 83 (2015) 229–247.
[19] G.B. Wallis, One-dimensional two phase flow, McGraw-Hill, New York, 1969.
[20] J.R. Thome Engineering Data Book III 2006 Wolverine Tube Inc. Void Fractions in Two Phase Flow.
[21] R. Clift J.R. Grace M.E. Weber Bubbles 2005 Dover Publications Inc, Mineola, New York Drops and Particles.
[22] S. Guet, G. Ooms, R.V.A. Oliemans, R.F. Mudde, Bubble size effect on low liquid input drift-flux parameters, Chem. Eng. Sci. 59 (2004) 3315–3329.
[23] T. Hibiki, M. Ishii, One-dimensional drift-flux model and constitutive equations for relative motion between phases in various two-phase flow regimes, Int. J. Heat Mass Tran. 46 (2003) 4935–4948.
[24] D.J. Nicklin, J.O. Wilkes, J.F. Davidson, Two phase flow in vertical tubes, Inst. Chem. Eng. 40 (1962) 61–68.
[25] S.Z. Rouhani, E. Axelsson, Calculation of void volume fraction in the subcooled and quality boiling regions, Int. J. Heat Mass Tran. 13 (2) (1970) 383–393.
[26] R.H. Bonnecaze, W. Erskine, E.J. Greskovich, Hold up and pressure drop for two phase slug flow in inclined pipelines, AIChE Journal 17 (1971) 1109–1113.
[27] E.J. Greskovich, W.T. Cooper, Correlation and prediction of gas–liquid holdups in inclined upflows, AIChE Journal 21 (1975) 1189–1192.
[28] S.L. Kokal, J.F. Stanislav, An experimental study of two-phase flow in slightly inclined pipes—II. liquid holdup and pressure drop, Chem. Eng. Sci. 44 (3) (1989) 681–693.
[29] A.R. Hasan, Void fraction in bubbly and slug flow in downward vertical and inclined systems, SPE Prod. Facil. 10 (3) (1995) 172–176.
[30] L.E. Gomez, O. Shoham, Z. Schmidt, R.N. Choshki, T. Northug, Unified mechanistic model for steady state two phase flow: horizontal to upward vertical flow, Soc. Petrol. Eng. J. 5 (2000) 339–350.
[31] J. Schmidt, H. Giesbrecht, C.W.M. van der Geld, Phase and velocity distributions in vertically upward high-viscosity two-phase flow, Int. J. Multiph. Flow 34 (2008) 363–374.
[32] J. Choi, E. Pereyra, C. Sarica, C. Park, J.M. Kang, An efficient drift-flux closure relationship to estimate liquid holdups of gas-liquid two-phase flow in pipes, Energies 5 (2012) 5294–5306.
[33] S. Evgenidis, T. Karapantsios, Effect of bubble size on void fraction fluctuations in dispersed bubble flows, Int. J. Multiph. Flow 75 (2015) 163–173.
[34] A. Chatzidafni, S. Evgenidis, I. Lioumbas, T. Karapantsios, Electrical Resistance Tomography in upward co-current bubbly flow, In: 4th Int. Workshop "Bubble and Drop Interfaces", Thessaloniki, Greece, 2009.
[35] S.P. Evgenidis, N.A. Kazakis, T.D. Karapantsios, Bubbly flow characteristics during decompression sickness: effect of surfactant and electrolyte on bubble size distribution, Colloids Surf. A: Physicochem. Eng. Aspects 365 (2010) 46–51.
[36] J. Schlegel, T. Hibiki, M. Ishii, Development of a comprehensive set of drift-flux constitutive models for pipes of various hydraulic diameters, Prog. Nucl. Ener. 52 (2010) 666–677.
[37] D. Rodrigue, Generalized correlation for bubble motion, A. I. Ch. E. J. 47 (2001) 39–44.
[38] R.P. King, Modeling and simulation of mineral processing systems, Butterworth-Heineman, London, 2001.
[39] S. Baz-Rodriguez, A. Aguilar-Corona, A. Soria, Rising velocity for single bubbles in pure liquids, Rev. Mex. Ing. Quim. 11 (2) (2012) 269–278.